would be expected to be less than for a graphite model since the pyrolysis vapors block a portion of the incident convective heating and since the combustion reaction of the vapors with the air in the boundary layer utilizes oxygen that would otherwise diffuse to the surface. Adjusting the surface-recession velocity to account for the "inert environment" contribution (i.e., subtracting the amounts due to shrinkage and due to oxidation by pyrolysis gases as determined from the surface-recession velocity measured in an inert environment), the velocities are below the level predicted for graphite using Eq. (3).[11]

References

[1] Vojvodich, N. S. and Pope, R. B., "Effect of Gas Composition on the Ablation Behavior of a Charring Material," *AIAA Journal*, Vol. 2, No. 3, March 1964, pp. 536–542.

[2] Clark, R. K., "Effect of Environmental Parameters on the Performance of Low-Density Silicone-Resin and Phenolic-Nylon Ablation Materials," TND-2543, Jan. 1965, NASA.

[3] Lundell, J. H., Dickey, R. R., and Jones, J. W., "Performance of Charring Ablative Materials in the Diffusion-Controlled Surface Combustion Regime," *AIAA Journal*, Vol. 6, No. 6, June 1968, pp. 1118–1126.

[4] Lundell, J. H., Wakefield, R. M., and Jones, J. W., "Experimental Investigation of a Charring Ablative Material Exposed to Combined Convective and Radiative Heating," *AIAA Journal*, Vol. 3, No. 11, Nov. 1965, pp. 2087–2095.

[5] Kelsey, J. R., "Calibration of the University of Texas Hyperthermal Tunnel," Aerospace Engineering Report 68002, June 1968, University of Texas at Austin, Austin, Texas.

[6] Hiester, N. K. and Clark, C. F., "Feasibility of Standard Evaluation Procedures for Ablating Materials," CR-379, Feb. 1966, NASA.

[7] Hiester, N. K. and Clark, C. F., "Comparative Evaluation of Ablating Materials in Arc Plasma Jets," CR-1207, Dec. 1968, NASA.

[8] Kratsch, K. M., Hearne, L. F., and McChesney, H. R., "Theory for the Thermophysical Performance of Charring Organic Heat-Shield Composites," Rept. 803099, Oct. 1963, LMSC.

[9] Scala, S. M. and Gilbert, L. M., "Sublimation of Graphite at Hypersonic Speeds," *AIAA Journal*, Vol. 3, No. 9, Sept. 1965, pp. 1635–1644.

[10] Boison, J. C. and Curtiss, H. A., "An Experimental Investigation of Blunt Body Stagnation Point Velocity Gradient," *ARS Journal*, Vol. 29, No. 2, Feb. 1959, pp. 130–135.

[11] Williams, J. R., Nipper, M. J., and Conine, W. D., "Comparative Performance of Phenolic Nylon in Arc-Heated Streams of Air and Nitrogen," Aerospace Engineering Research Report 69002, May 1969, University of Texas at Austin, Austin, Texas.

Nozzle Boundary-Layer Displacement Thickness at Mach Numbers 30 to 70

Charles G. Miller*
NASA Langley Research Center, Hampton, Va.

Nomenclature

$(A/A^*)_{eff}$ = ratio of effective nozzle-to-throat cross-sectional area (mass flow considerations)
$(A/A^*)_{geo}$ = ratio of geometric nozzle-to-throat cross-sectional area
d^* = nozzle throat diameter
M_∞ = freestream Mach number
$p_{t,1}$ = reservoir pressure
p_∞ = freestream static pressure
$R_{\infty,x}$ = freestream Reynolds number based on axial distance from nozzle cone apex
$T_{t,1}$ = reservoir temperature
T_∞ = freestream static temperature
x = axial distance from nozzle cone apex
δ^* = boundary-layer displacement thickness
γ_∞ = freestream ratio of specific heats
θ = nozzle-divergence half-angle

Received May 7, 1969; revision received July 31, 1969.
* Aerospace Engineer, Special Projects Section, Aero-Physics Division. Member AIAA.

Introduction

Over the past decade, the empirical relations of Refs. 1 and 2 for predicting hypersonic nozzle boundary-layer displacement thickness in air have received considerable usage. More recently, a similar study in nitrogen (Ref. 3) showed that extrapolation of the empirical relations of Refs. 1 and 2 to Mach numbers greater than those from which they were obtained resulted in overestimation of the nozzle displacement thickness. An empirical relation employing the same parameters used in Refs. 1 and 2 was derived by Whitfield and presented by Edenfield in Ref. 3. This relation was obtained from higher Mach number data so as to more accurately predict hypersonic nozzle displacement thickness for Mach numbers to approximately 20. The present study provides preliminary nozzle displacement thickness results in helium at Mach numbers much greater than those of the aforementioned hypersonic studies. These results, obtained in the Langley hotshot tunnel, include the effects of wide ranges of reservoir pressure, reservoir temperature, and geometric area ratio. An empirical relation for predicting nozzle displacement thickness over the present range of Mach numbers (30 to 70) is presented.

Apparatus and Tests

A description of the Langley hotshot tunnel is presented in Ref. 4. As mentioned in Ref. 4, this facility employs a 10° total-divergence angle conical nozzle. The present helium results, which represent part of a recent calibration study, were obtained for a reservoir pressure range of 3000 to 23,000 psi and reservoir temperature range of 1500° to 11,000°R. These reservoir conditions, in conjunction with variation in nozzle-throat diameter, resulted in Mach numbers of 30 to 70 and Reynolds numbers of 4×10^5 to 5×10^6/ft.

Results and Discussion

Pitot pressure surveys in the nozzle test section showed, in general, that the pitot pressure was essentially constant across the inviscid core. A value of the effective-area ratio $(A/A^*)_{eff}$ corresponding to the mean of the measured pitot pressures across the core, was determined from mass flow considerations.[5] Assuming the displacement thickness at the nozzle throat to be zero, the nozzle displacement thickness was obtained from the nondimensional expression

$$\delta^*/x = \tan\theta - (d^*/2x)[(A/A^*)_{eff}]^{1/2} \quad (1)$$

Figure 1 shows the effect of reservoir pressure on nozzle displacement thickness for a given geometric area ratio of 2.03×10^4 ($d^* = 0.150$ in. and $x = 122$ in.) and reservoir temperature of approximately 3800°R. The nozzle displacement thickness is observed to decrease approximately 27% [$\Delta(\delta^*/x) = -0.013$] as the reservoir pressure increases nearly eightfold from 3000 to 23,000 psi. For this change in $p_{t,1}$, there was an accompanying increase in M_∞ from 41 to 50 and in $R_{\infty,x}$ from 4.3×10^6 to 2.25×10^7. As shown in Fig. 1, the empirical relations of Refs. 1 and 2, in terms of M_∞ and $R_{\infty,x}$, predicted values of δ^*/x approximately twice those of the present data and Ref. 1 failed to predict the trend of decreasing δ^*/x with increasing $p_{t,1}$. The empirical relation derived by Whitfield and presented by Edenfield in Ref. 3 underestimated the present data by approximately $\frac{1}{3}$, but predicted the trend accurately. For the case of hypersonic flow over a flat plate, the displacement thickness in air is about $\frac{3}{5}$ that in helium for the same value of Mach number

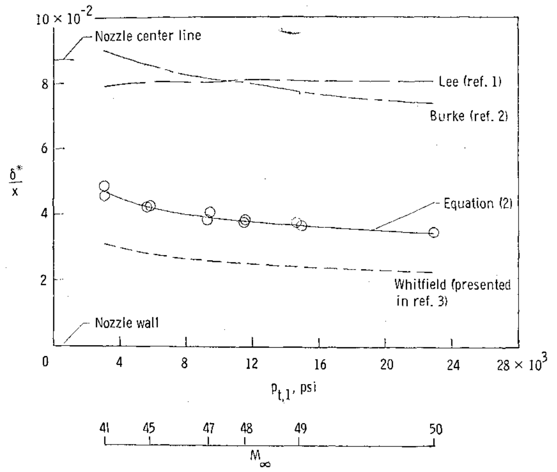

Fig. 1 Variation of nozzle boundary-layer displacement thickness with reservoir pressure. $T_{t,1} \approx 3800°R$, $d^* = 0.150$ in., $x = 122$ in.

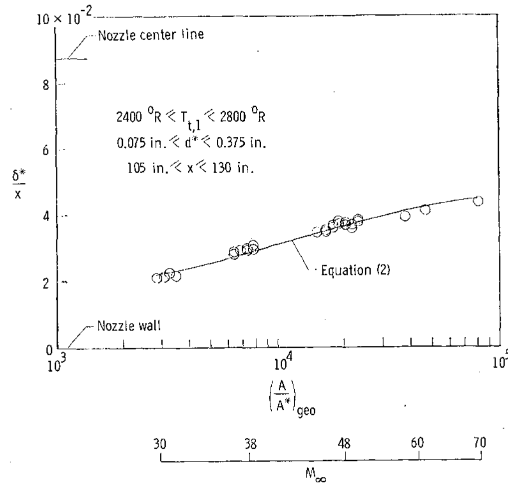

Fig. 3 Variation of nozzle boundary-layer displacement thickness with geometric area ratio.

and Reynolds number.[6] This air-helium simulation factor of $\frac{3}{5}$ is surprisingly close to the ratio of $\frac{2}{3}$ observed between the prediction of Whitfield and the present data.

Since thd relation of Whitfield predicted the trend of the present results, it was decided to modify the constant of this relation to bring the prediction into agreement with the present data. To account for the difference in γ_∞ between the present study and that of Whitfield, a linear variation in the constant as a function of γ_∞ was assumed, resulting in the expression

$$\delta^*/x = (0.435\, \gamma_\infty - 0.389)\, M_\infty^{1/2}/(R_{\infty,x})^{1/4} \qquad (2)$$

As shown in Fig. 1, Eq. (2) satisfactorily predicts δ^*/x for the entire range of $p_{t,1}$; discretion should be used, however, in the application of Eq. (2) at conditions other than those of Whitfield for air or nitrogen and those of the present helium study.

The effect of reservoir temperature on nozzle displacement thickness is shown in Fig. 2 for $(A/A^*)_{geo} = 2.03 \times 10^4$ and $p_{t,1} \approx 9200$ psi. The nozzle displacement thickness is observed to increase approximately 45% $[\Delta(\delta^*/x) = 0.015]$ as the reservoir temperature increases nearly sevenfold from 1500° to 11,000°R. For this increase in $T_{t,1}$, there was an accompanying decrease in M_∞ from 51 to 41 and in $R_{\infty,x}$ from 2.7×10^7 to 4.1×10^6. Again, the empirical relations of Refs. 1 and 2 overestimated δ^*/x by a factor of approximately 2 and the relation of Whitfield presented by Edenfield in Ref. 3 underestimates the present data by approximately $\frac{1}{3}$. Equation (2) is observed to yield a good prediction of δ^*/x for the present $T_{t,1}$ range.

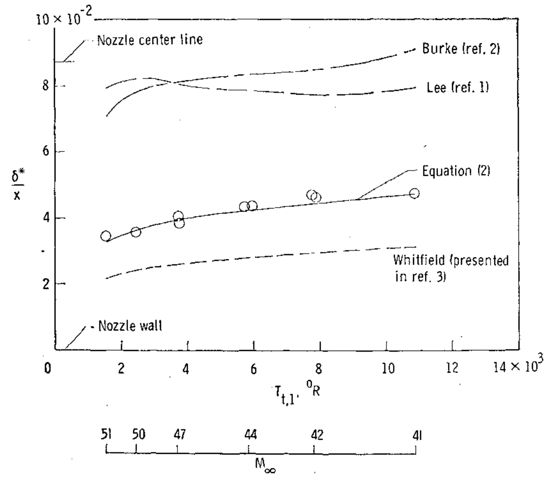

Fig. 2 Variation of nozzle boundary-layer displacement thickness with reservoir temperature. $P_{t,1} \approx 9200$ psi, $d^* = 0.150$ in., $x = 122$ in.

Figure 3 presents the variation of nozzle displacement thickness with geometric area ratio where the variation in $(A/A^*)_{geo}$ represents nozzle-throat diameters from 0.075 to 0.375 in. and axial stations from 105 to 130 in. The data were obtained for reservoir temperatures of 2400° to 2800°R, and for $(A/A^*)_{geo} < 3 \times 10^4$, $p_{t,1} \approx 11{,}500$ psi, whereas for $(A/A^*)_{geo} > 3 \times 10^4$, $p_{t,1} \approx 15{,}000$ to 17,500 psi. The results presented in Fig. 3 represent a M_∞ range of 30 to 70 and $R_{\infty,x}$ range of 1.6×10^7 to 4.7×10^7. The displacement thickness is observed to increase over 100% as $(A/A^*)_{geo}$ increases from 2.8×10^3 to 8.1×10^4. Equation (2) is observed to predict values of δ^*/x to within $\pm 10\%$ over the M_∞ range 30 to 70.

A real-helium expression for nozzle displacement thickness in terms of the nozzle geometric parameters, reservoir conditions, and freestream Mach number may be derived from Eq. (2). Assuming ideal-helium behavior in the freestream and employing the viscosity relation of Ref. 7, Eq. (2) may be expressed as

$$\delta^*/x = C_0(M_\infty T_\infty^{1.147}/x p_\infty)^{1/4} \qquad (3)$$

where C_0 is a constant. Now p_∞ and T_∞ can both be related to $p_{t,1}$ and $T_{t,1}$ for real helium by use of the equations in the Appendix of Ref. 5. The required ideal helium expressions in terms of M_∞ are presented in Ref. 8. The final expression is

$$\frac{\delta^*}{x} = C_1 \left[\frac{M_\infty(M_\infty^2+3)^{1.353}\,(AT_{t,1})^{1.147}}{xBp_{t,1}}\right]^{1/4} \qquad (4)$$

where the real-helium correction factors A and B are given by

$$A = 1 + p_{t,1}\left(\frac{0.7901}{T_{t,1}^{1.3628}} - \frac{2.4311 \times 10^1}{T_{t,1}^{2.1286}}\right)$$

$$B = 1 + p_{t,1}\left(\frac{1.4538}{T_{t,1}^{1.3640}} - \frac{1.3801 \times 10^3}{T_{t,1}^{2.8233}}\right)$$

and $p_{t,1}$ is in atm, $T_{t,1}$ in °K, x in ft, and $C_1 = 1.1346 \times 10^{-3}$. For ideal helium, $A = B = 1$.

References

[1] Lee, J. D., "Axisymmetric Nozzles for Hypersonic Flows," TN (ALOSU) 459-1 (WADC TN 59-228), June 1959, Ohio State Univ. Research Foundation.

[2] Burke, A. F., "Turbulent Boundary Layers on Highly Cooled Surfaces at High Mach Numbers," *Proceedings of Sympos-*

ium on Aerothermoelasticity, ASD TR 61-645, U. S. Air Force, 1961, pp. 704–741.

[3] Edenfield, E. E., "Contoured Nozzle Design and Evaluation for Hotshot Wind Tunnels," AIAA Paper 68-369, San Francisco, Calif., 1968.

[4] Miller, C. G., III, Creel, T. R., Jr., and Smith, F. M., "Calibration Experience in the Langley Hotshot Tunnel for Mach Numbers from 12 to 26," TN D-3278, 1966, NASA.

[5] Miller, C. G., III and Wilder, S. E., "Real-Helium Hypersonic Flow Parameters for Pressures to 3600 Atmospheres and Temperatures to 15,000°K," TN D-4869, 1968, NASA.

[6] Love, E. S., Henderson, A., Jr., and Bertram, M. H., "Some Aspects of Air-Helium Simulation and Hypersonic Approximations," TN D-49, 1959, NASA.

[7] Keesom, W. H., *Helium,* Elsevier, New York, 1942, pp. 104–107.

[8] Mueller, J. N., "Equations, Tables, and Figures for Use in the Analysis of Helium Flow at Supersonic and Hypersonic Speeds," TN 4063, 1957, NACA.

Optimal Linear Regulators with Exponentially Time-Weighted Quadratic Performance Indices

F. T. MAN*

University of Toronto, Toronto, Ontario, Canada

Introduction

ONE of the performance indices used in the classical design of single-input and single-output linear time-invariant systems is the integral of exponentially time-weighted squared error. This type of performance indices heavily penalizes long-duration errors and hence tends to give designs that yield well-damped responses. The use of exponentially time-weighted performance indices has been in later years revived by Kalman et al.,[1] Tyler,[2] and Sage[3] in the design of optimal linear regulators. The solution of this optimal linear regulator problem for finite terminal time is straightforward[2,3] and differs only slightly from that of the conventional problem. The solution for this particular problem for infinite terminal time, however, is not as trivial and is not available in literature. It is the intent of this Note to present a solution for the linear regulator problem optimal for exponentially time-weighted quadratic performance indices. The method of solution utilizes the concept of cost equivalence, to be defined in the next section, in conjunction with the theory of optimal linear regulator.

Concept of Cost Equivalence

For the sake of convenience, a linear time-invariant asymptotically stable system $\dot{y} = Fy$ and its associated quadratic cost functional

$$J = \int_0^\infty y'Pydt$$

will be denoted by $[F,P]$. The representation $[F_1,P_1]$ is said to be cost-equivalent to $[F_2,P_2]$ if F_1 and F_2 are stability matrices, P_1 and P_2 are nonnegative symmetric matrices and $J_1 = J_2$. Based on this notation and definition, the following result can be deduced immediately without proof.

Lemma: $[F,e^{2\lambda t}P]$ is cost equivalent to $[F + \lambda I,P]$ for any λ, if both representations possess the same initial conditions, and the equivalence is one-to-one correspondent.

Received June 23, 1969. This work was supported by a National Research Council of Canada scholarship.

* Graduate Student, Department of Electrical Engineering.

It should be emphasized that, although the two representations are cost-equivalent, they are not equivalent in the sense of Lyapunov,[4] and their trajectories are related by the nonsingular transformation $e^{\lambda t}I$. Since the optimal linear regulator problem is concerned primarily with the minimization of the cost of a system rather than the shape of the trajectory of the system, the concept of cost equivalence will be useful in the development of the main result of the Note.

Main Result

Consider a linear time-invariant controllable system

$$\dot{x} = Ax + Bu,\ x(0) = x_0 \tag{1}$$

and a quadratic cost functional

$$J = \int_0^\infty e^{2\sigma t}(x'Qx + u'Ru)dt \tag{2}$$

where A, B, Q, and R are constant matrices of compatible dimensions and appropriate definiteness, and σ is an arbitrary positive constant. The problem of interest is to find an optimal control law such that (2) is minimized subject to (1). Because the integrand of (2) is unbounded when the terminal time approaches infinity, the method of derivation of the conventional optimal linear regulator cannot be directly employed without some prior mathematical modifications. With the use of the concept of cost equivalence, it is possible to state and prove the following result.

Theorem: The optimal control law which minimizes (2) subject to (1) is given by

$$u^* = -R^{-1}B'Sx \tag{3}$$

where the symmetric matrix S is the unique positive definite solution of the algebraic matrix Riccati equation

$$A'S + SA + 2\sigma S - SBR^{-1}B'S + Q = 0 \tag{4}$$

Moreover, the real parts of all the eigenvalues of the resulting closed-loop system $(A - BR^{-1}B'S)$ are less than $-\sigma$.

Proof: It is well known that if (A,B) is a controllable pair, $(A + \sigma I,B)$ is also controllable for any σ. From a result by Wonham,[5] there always exists a feedback control law of the form

$$u = -Kx \tag{5}$$

such that $(A + \sigma I - BK)$ is a stability matrix, that is, the real parts of all the eigenvalues of $(A - BK)$ are less than $-\sigma$. Applying (5) to (1) and (2) gives $[A - BK,e^{2\sigma t}(Q + K'RK)]$, which, in view of the previous lemma, is equivalent to $[A + \sigma I - BK,Q + K'RK]$ in which

$$\dot{z} = (A + \sigma I - BK)z,\ z(0) = x_0 \tag{6}$$

$$J = \int_0^\infty z'(Q + K'RK)zdt \tag{7}$$

Using now the conventional theory of optimal linear regulator, the control law that minimizes (7) subject to (6) is given by

$$\hat{u} = -R^{-1}B'Sz \tag{8}$$

where the symmetric S is given by (4). Furthermore, the matrix $(A + \sigma I - BR^{-1}B'S)$ is asymptotically stable, and, consequently, the real parts of all the eigenvalues of the closed-loop system are less than $-\sigma$.

It should be noted that the optimal control law of (8) is a linear feedback of the vector z instead of the state vector x. To complete the proof of the theorem, it is required to show that both (3) and (8) result in identical costs. Applying (3) to (1) and (2) leads to $[A - BR^{-1}B'S,e^{2\sigma t}(Q + SBR^{-1}B'S)]$ which, with the use of the previous lemma, is equivalent to $[A + \sigma I - BR^{-1}B'S,Q + SBR^{-1}B'S]$. Indeed, the latter is the optimum representation of (6) and (7), and hence (3) is the optimal control law minimizing (2) subject to (1).